Microchimica Acta (2023) 190:90
https://doi.org/10.1007/s00604-023-05680-8

ORIGINAL PAPER

Chitosan/luminol/AgNPs nanocomposite for electrochemiluminescent determination of prostate-specific antigen

Hassan Nasrollahpour[1,2] · Balal Khalilzadeh[3] · Abdolhossein Naseri[1] · Shahab Mamaghani[4] · Ibrahim Isildak[5] · Mohammad-Reza Rashidi[6]

Received: 31 August 2022 / Accepted: 30 January 2023 / Published online: 14 February 2023

Abstract

A green, environmentally friendly protocol was developed for ultrasensitive and highly specific recognition of prostate-specific antigen (PSA) based on the ECL effect of luminol supported by chitosan-silver nanoparticles (CS/AgNPs) nanocomposites. The transducing surface was fabricated through two consecutive electrodeposition steps of gold nanoparticles (AuNPs) and chitosan (CS)-AgNPs-luminol electrochemiluminophore onto the glassy carbon electrode. In addition to an appropriate desirable biocompatibility, the electrochemical synthesis presents low-cost preparation and ultrafast determination opportunity. AgNPs play a linking role to attach luminol, as an ECL agent to the CS support via donor-acceptor bonds between Ag atoms with NH groups of luminol and CS. Also, AgNPs can amplify the ECL intensity as a consequence of their excellent specific surface area and conductivity. To enhance the performance of the nanobiosensor, AuNPs were also used due to their high-specific surface area and excellent affinity toward amine groups of CS. Based on this high-performance analysis strategy, ultrasensitive screening of PSA was attained with a desirable limit of detection of 0.6 ng mL^{-1} and a broad linear range between 1 pg mL^{-1} and 10 ng·mL^{-1} (R^2=0.994). Approximately, the same results were recorded for the analysis of the unprocessed serum samples of patients with prostate cancer at different stages. This research provided significant insight into electrografting methods to construct ECL transducers for clinical monitoring of PSA and other tumor biomarkers in the clinical setting.

Keywords Electrochemiluminescnece · Prostate-specific antigen · Gold nanoparticles · Nanobiocomposite · Biosensor · Electrodeposition

Introduction

Electrochemiluminescence (ECL) is a photon-induced process accompanied by a luminescence molecule that experiences an electrochemical redox reaction onto the electrode surface [1]. In recent years, the rapidly growing domain of nanotechnology has substantially benefited electrochemiluminescence (ECL) technology by boosting photon-induced reactions, signal stability, and applicability via the utilization of discrete characteristics of various nanostructures [2]. Several nanomaterials with different natures, sizes, shapes, and luminescence features have been employed in ECL biosensing development [3–6]. These nanomaterials may have a luminescence property or accelerate the ECL phenomenon to reach higher quantum yields [7]. Our group employed reduced graphene oxide (rGO) to enhance the ECL signals by $Ru(bpy)_3^{2+}$ for the analysis of breast cancer serum samples. In this

✉ Balal Khalilzadeh
balalkhalilzadeh@gmail.com; khalilzadehb@tbzmed.ac.ir

1 Department of Analytical Chemistry, Faculty of Chemistry, University of Tabriz, Tabriz, Iran

2 Cancer Research Center, Shahid Beheshti University of Medical Sciences, Tehran, Iran

3 Stem Cell Research Center, Tabriz University of Medical Sciences, Tabriz 51664-14766, Iran

4 Department of Dermatology, University Hospital of Zurich, Zurich, Switzerland

5 Department of Bioengineering, Faculty of Chemistry-Metallurgy, Yildiz Technical University, 34220 Istanbul, Turkey

6 Department of Medicinal Chemistry, Faculty of Pharmacy, Tabriz University of Medical Sciences, Tabriz, Iran

strategy, rGO enhanced the loading capacity and also the attachment ability of the lumnophore on the electrode [8]. Wang et al. developed an ECL biosensor for the detection of miRNA-141. They used reduced graphene oxide/Au nanoparticles (rGO/NPs) and AuPd NPs to accelerate N-(4-aminobutyl)-N-(ethylisoluminol) (ABEI)/H_2O_2 ECL system. The proposed nanobiosensor could detect miRNA-141 as low as 31.9 aM [9]. Huang and coworkers introduced an aptasensing of MUC-1 protein. The protocol relied on zinc meso-tetra(4-sulfonatophenyl) porphine (Zn-TP) as electrochemiluminophore and Zn-based metal-organic frameworks with pyridine (Zn-Bp-MOFs) as ECL enhancer. After the combination of Zn-Bp-MOFs and Zn-TP, the obtained nanostructure was deposited onto the working electrode. The ECL signals were increased by 32 times more than Zn-TP alone. $K_2S_2O_8$ was also used as a co-reactant to enhance the ECL. The method represented a high LOD of 0.23 pg mL^{-1} for detecting MUC-1 [10]. In another research, Rebeccani et al. utilized carbon nanotubes (CNTs) to boost ECL emission of $[Ru(bpy)_3]^{2+}$. CNTs are conductive materials that fasten the electrode surface's electron transferring rate and boost ECL signals. An increase of ~4 magnitudes was obtained In ECL readouts [11]. Biosensors have critical role in the early-stage diagnosis of most types of cancers, neurodegenerative diseases, stem cell biology, and also in differentiation [12–17].

Prostate-specific antigen (PSA) is secreted by prostatic epithelial cells and is a single-chain glycoprotein [18]. Early-stage monitoring of PSA levels in serum can increase the survival rate and treatment efficiency in patients with prostate cancer [19]. To this end, tremendous efforts have been done in the development of biosensing strategies for PSA detection using ECL assays. Owning to the advantages and properties described for ECL-based strategies, trace levels of PSA can be measured in the early stage of prostate gland disorders [20]. However, the healthcare utility of these ECL systems to recognize prostate cancer have several shortages prevent them for miniaturization and commercialization. The imparting luminohpores to the trasducing surfaces is a key parameter which could answer many of the current challenges. This step affect the accuracy, stability, repeatability, and consumed time of the designed systems. Therefore, the development of new methods to approach commercialization of the bioelectronic tools for on-site, rapid, and reliable PSA assessment in biological fluids needs to be addressed.

Among some frequently used ECL emitters, such as Ru $(bpy)_3^{2+}$, luminol, and transition metal quantum dots, luminol and its derivatives have attracted tremendous attitudes with specific features such as high quantum yields, acceptable stability, and easy availability [21–23]. In this research, we implemented an ECL biosensor capable of PSA recognition in serum samples of patients with prostate cancer. In this regard, for the first time we used an electrochemical deposition methodology as a green, time-effective, and highly repeatable strategy to prepare a novel ECL system, chitosan-silver nanoparticles-luminol (CS-AgNPs-Lu). AgNPs are employed as linkers between CS and luminol via Ag-NH interactions. In contrast to previously reported ECL frameworks based on luminol composites, the proposed platform has several advantages including but not limited to the following: (i) CS is a biocompatible polymer with excellent attachability, functionality, and stability in high and low potentials; (ii) AgNPs increase the luminescence of luminol by binding it to CS and also boost the charge transferring on the electrode surface leading to higher ECL quantum yield; (iii) most importantly, the electrodeposition strategy used for grafting luminol on the electrode present many tremendous benefits including decreased deposition time, stability, increase the repeatability, and reliability of the framework. The produced framework was then employed for the analysis of PSA in untreated PSA-positive sera.

Experimental

Materials

PSA antibody (Ab) and PSA were obtained from Abcam. CS powder and luminol were purchased from Merck. $AgNO_3$ salt was acquired from Sigma-Aldrich. Phosphate buffer (PB, pH= 7.4) was prepared by dissolving 200 mg KCl, 1.44 g Na_2HPO_4, 8 g NaCl, and 245 mg KH_2PO_4, in the double-distilled water (DDW) under ambient conditions. All salts utilized in this study were purchased from Merck.

Instrumental

A Metrohm Autolab system and Nova software were used for all the electrochemical measurements. A commonly used three-electrode system was employed for all the experiments, which included a gold electrode (AuE) (diameter = 2 mm) as the working electrode, a Pt wire as the counter electrode, and an Ag/AgCl electrode as the reference electrode. All the ECL experiments were performed by utilizing a homemade ECL instrument with a photomultiplier transducer (PMT, Hamamatsu, Japan) at a wavelength of 450 nm. The ECL results were recorded through a homemade interface coupled with Autolab. All analyses were performed under ambient conditions. An ultrasonic bath (Model: 420; Transsonic) was utilized to homogenize the solutions before use. The pH of solutions was adjusted via a pH meter (Corning, model 120). Scanning electron microscope (SEM) images, electron dispersive X-ray spectroscopy (EDX), and dot mapping were

recorded by a Tescan instrument (Model: MIRA3). UV–Vis absorption spectra were obtained by employing a UV–Vis spectrophotometer (Shimadzu UV-2550).

Methods

Stepwise preparation of CS/AgNPs-luminol

The luminol/AgNPs nanocomposite was successfully synthesized according to the previously reported procedures with some modifications [24–26].

Electrodeposition of AuNPs and chitosan/luminol/AgNPs

Electrochemical precipitation of AuNPs was performed on the gold electrode using chronoamperometry (−0.5 V) in a solution containing $HAuCl_4$ (1 mM) and H_2SO_4 (0.5 M). After rinsing the electrode with distilled water, the AuNPs-modified electrode was placed into the as prepared CS/AgNPs/Lu solution (under light-protected conditions). Afterward, the CS/AgNPs/Lu nanocomposite was deposited onto the AuNPs-modified gold electrode via chronoamperometry (−2.5 V, for 80 s). The electrode was then rinsed with ultrapure water and employed for PSA analysis.

PSA detection procedure

After electrodeposition of AuNPs and chitosan/luminol/AgNPs nanocomposite onto the working electrode (CS/AgNPs/Lu-AuNPs-AuE), 10 µL of streptavidin solution (10 µg mL^{-1}) was incubated onto the modified gold electrode denoted as Str-CS/AgNPs/Lu-AuNPs-AuE. In the following, a 10 µL biotinylated monoclonal anti-PSA antibody (10 µg mL^{-1}) was drop-casted onto Str-CS/AgNPs/Lu-AuNPs-AuE denoted as Ab-Str-CS/AgNPs/Lu-AuNPs-AuE and incubated at 8°C for 1 h. The electrode was then washed with distilled water and finally, a 10 µL PSA protein solution was drop-casted on the modified electrode and rested for 2 h.

Results and discussion

Electrode preparation steps

ECL method was employed to screen the stepwise preparation of the proposed framework. As for the ECL investigation, the cyclic voltammetry (CV) and ECL of each modification stage including CS/AgNPs/Lu-AuNPs-AuE, Str-CS/AgNPs/Lu-AuNPs-AuE, Ab-Str-CS/AgNPs/Lu-AuNPs-AuE, and PSA-Ab-Str-CS/AgNPs/Lu-AuNPs-AuE were assessed in 10 mL PB solution containing 50 µL H_2O_2 (30% solution in H2O) in the potential range of −0.15 to 0.45 V with a scan rate of 0.1 V/s. The transmission wavelength of PMT was set at 450 nm. As revealed in Fig. 1, a strong and stable ECL emission was observed after electrodeposition of the CS/AgNPs/Lu nanocomposite, and this value declined after incubation of Str/Ab, and PSA in a logical manner. These resulted from the steric hinderance of the Str, Ab, and PSA which prevented H_2O_2 from reaching to the electrode surface where it could rreact with luminol. To evaluate the impact of the electrodeposited AuNPs on the signals' quality, two discrete immunosensors were prepared in the presence and absence of electrodeposited AuNPs. Figure 2 represents the 8 repetitive ECL readouts for both fabricated platforms. The signal stability was dramatically boosted after electrodeposition of AuNPs. This could be correlated to the increased specific surface area after the electrodeposition of AuNPs, resulting in the enhancement of loading and attaching capability of CS/AgNPs/Lu nanocomposite onto the AuE.

UV–Vis evaluation

UV–Vis spectrum is a nice instrument to study and monitor the formation of nanomaterials via the location and/or intensity alteration of absorption bands. In this context, three previously prepared solutions including CS (4 mg mL^{-1}), CS-AgNPs, luminol, and CS-AgNPs-Lu were screened using UV–Vis spectrometry. Water was used as a blank solvent to correct background noises. CS-AgNPs-Lu mixture was used in two different dilutions. Also, CS-AgNPs were prepared as same as CS-AgNPs-luminol but without luminol addition and were diluted by 4 times before UV–Vis monitoring. In Figure S1, an intense absorption band below about 420 nm appeared after the formation of AgNPs. The peak intensity (absorbance) declined after the addition of luminol. This effect would be associated with the linkage of luminol to Ag atoms and the change in the absorption quality of AgNPs. The presence of luminol was also confirmed via two bands at 295 and 355 nm which are observed for both luminol and CS-AgNPs-luminol but with different intensities. The physicochemical properties of CS-AgNPs nanocomposites were relatively similar to the other studies [24, 26].

Morphological studies

To further evaluate the as-fabricated nanobiosensor, morphological studies were performed using SEM, EDX, and dot mapping analyses. Figure 3 represents the obtained SEM images with AuNPs-GCE and Lum/AgNPs/CS-AgNPs-GCE electrodes. Data showed that the nanoscale-sized particles in the deposited matrix in electrodes could be associated with AuNPs and AgNPs structures. The two

modified surfaces are different in terms of structure and morphology, indicating the successful deposition of the Lum/AgNPs/CS nanocomposite. Furthermore, to confirm the results of SEM, EDX quantitative elemental analysis, and dot mapping techniques were also done. Data revealed that two different compositions were found on AuNPs-GCE and Lum/AgNPs/CS-AgNPs-GCE electrodes, showing appropriate electrodeposition of the emitting nanocomposite on the electrode surface.

Optimization of the experimental conditions

To obtain the best results with the proposed nanobiosensor, the experimental conditions were optimized in several steps.

Optimizing the electrodeposition time of AuNPs

According to data from "Electrode preparation steps," the electrodeposited AuNPs have a significant effect on the stability and intensity of ECL response. To achieve more benefits from AuNPs on framework performance, the electrodeposition time was investigated. To this end, four different deposition times (30, 100, 150, and 200 s) were examined at the same analysis conditions (10 mL PB, 50 µL H_2O_2, pH=7.4, −0.5 V). Results indicated that ECL intensity was increased from 30 to 150 s after the electrodeposition of AuNPs (Figure S2). The further increase of electrodeposition time has no positive effect on the performance. It can be told that the loading capacity and surface-to-volume ratio were stimulated after increasing electrodeposition time from 30 to 150. At this time interval, the amounts of the nanobiocomposite loaded onto the electrode were increased, resulting in higher ECL intensity. Increasing electrodeposition time by more than

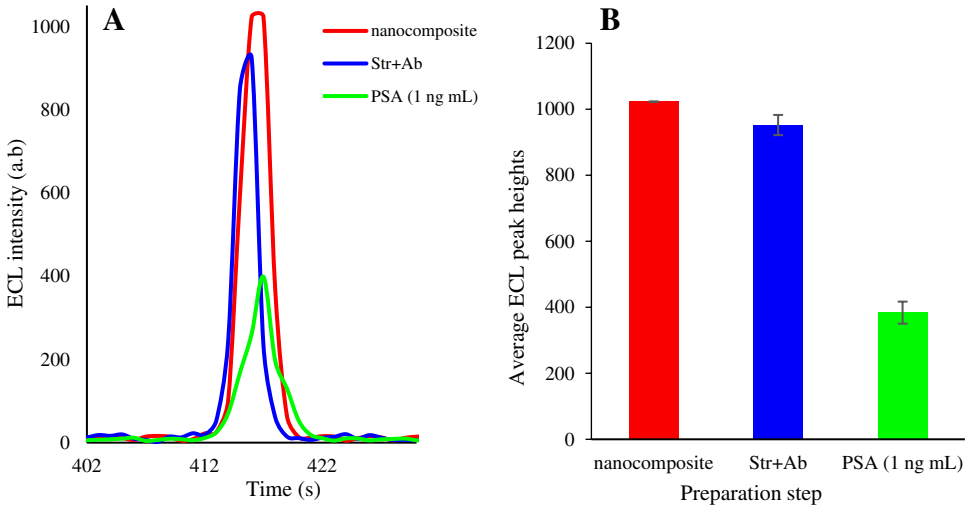

Fig. 1 ECL characterization of the preparation steps of the proposed immunosensor. **A** ECL graphs and **B** the correlated histograms (n=3)

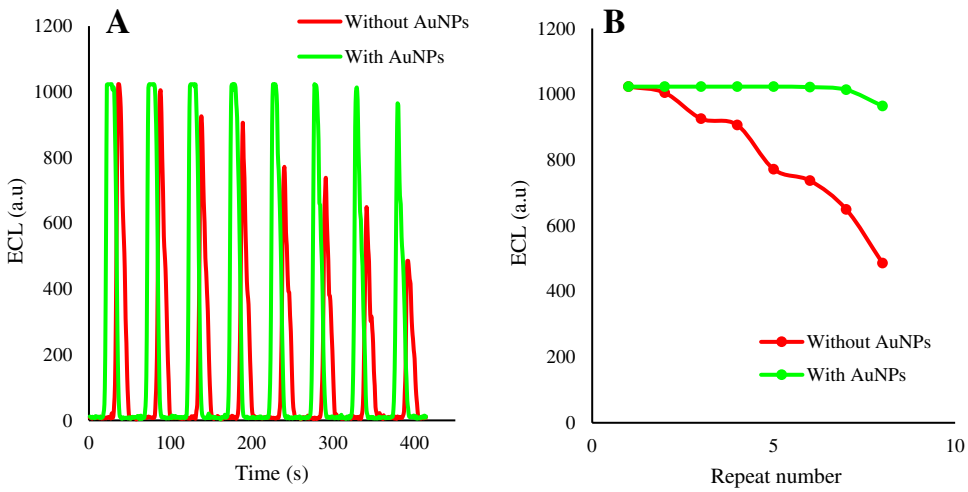

Fig. 2 The investigation of the effect of AuNPs on signal stability of the proposed ECL system. **A** 8 obtained consecutive ECL signals and **B** the dot-plotted graph

150 s could not enhance the loading capacity of nanocomposite and then no obvious change in ECL readouts was observed. As a result, the 150 s was selected as an optimum deposition time for the next experiments.

Optimizing the electrodeposition time of CS/AgNPs/luminol

In the next step, the electrodeposition time of the nanocomposite was assessed. In this regard, five electrodeposition times (20, 40, 80, 150, and 300 s) were tested at the same conditions (10 mL PB, 50 µL H_2O_2, pH=7.4, −2.5 V) and with the previously optimized deposition time used for AuNPs (150 s). As represented in Figure S3, the ECL readouts are stimulated with the electrodeposition time of CS/AgNPs/Lu. The ECL signal during the first 80 s reaches maximum levels at and then remained approximately constant as the time increased. This could be correlated with the loading amount of CS/AgNPs/Lu which enhances as the time raise from 20 to 80.Consequently, the 80 s was selected as an optimum electrodeposition time for CS/AgNPs/Lu nanocomposite.

Analytical performance

Calibration plot

The proposed ECL strategy was utilized for the recognition of PSA under the optimal experimental conditions. For this purpose, five PSA standard solutions were analyzed by the as-fabricated biosensor. According to the results, the ECL signal is decreased by reducing the concentration of PSA to 10 pg Ml^{-1}. This phenomenon indicates that the constructed framework presents a high sensitivity for the detection of PSA. In addition, the ECL signal is declined with the increasing concentration of PSA. As can be seen from Fig. 4, an appropriate linear relationship was obtained between the ECL response and the logarithmic concentrations of PSA.

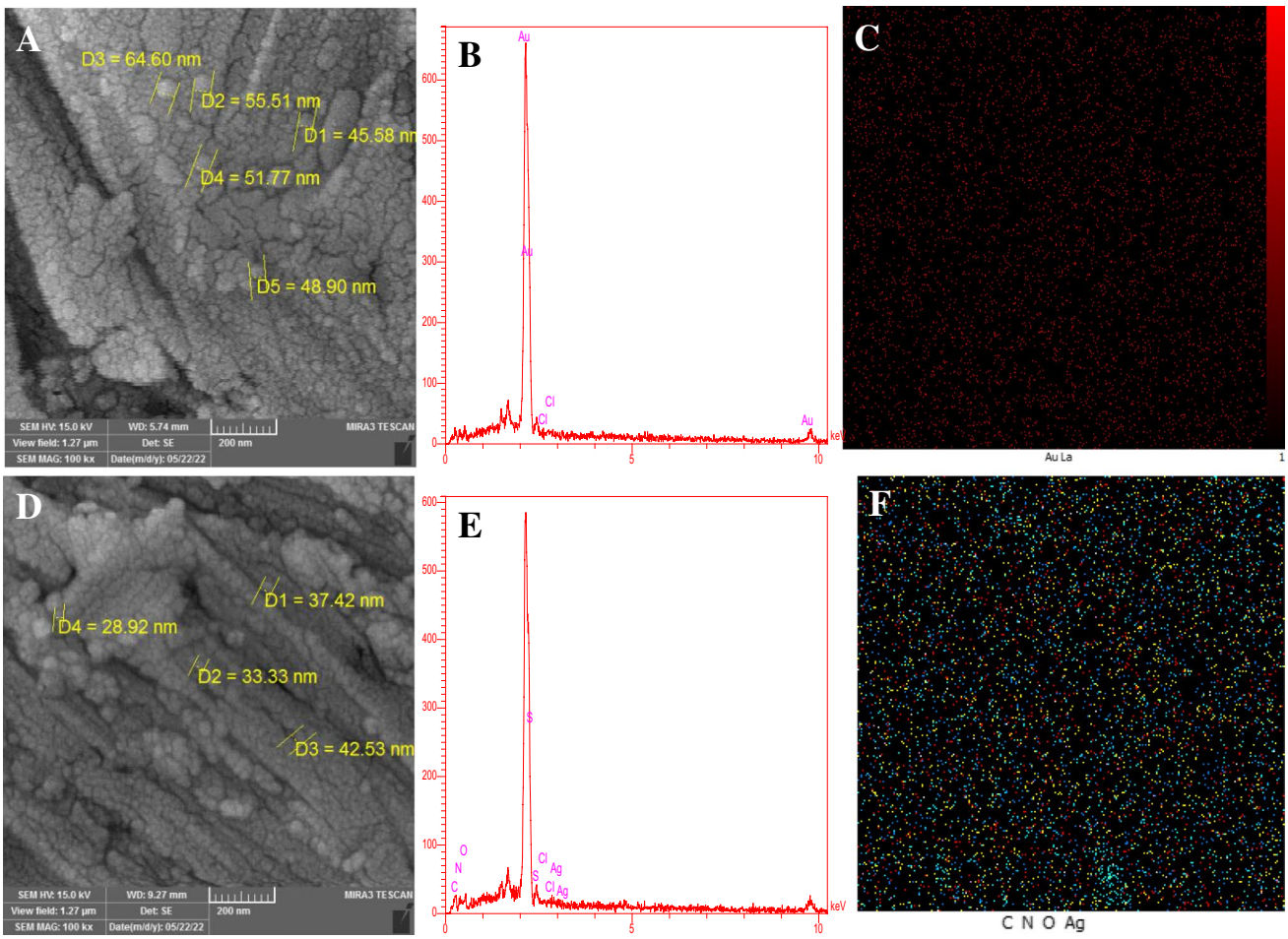

Fig. 3 Morphological studies of the proposed flamework onto the working electrode. **A**, **B**, **C** SEM images, EDX analysis, and dot mapping analysis of the AuNPs-modified GCE (AuNPs-GCE), respectively. **D**, **E**, **F** SEM images, EDX analysis, and dot mapping analysis of the Lum/AgNPs/CS-AuNPs-GCE, respectively (blue dots: Ag, red dots: N, yellow dots: C

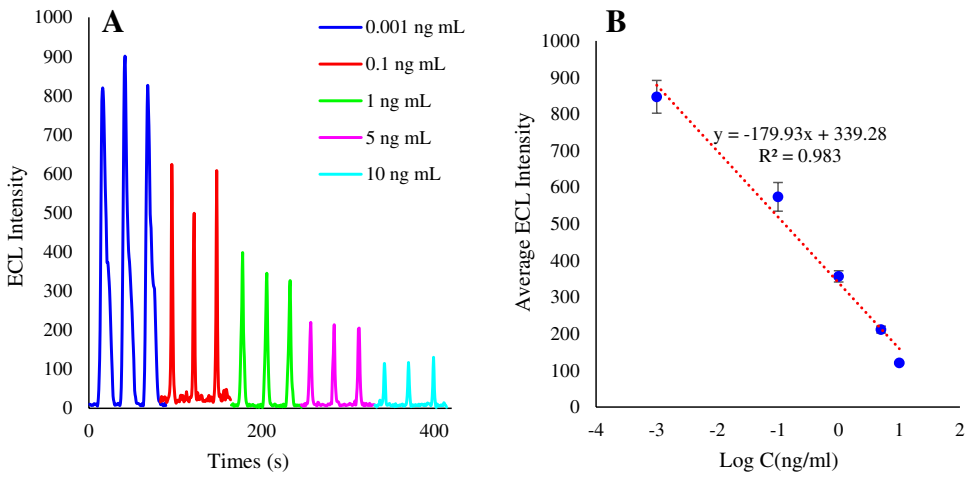

Fig. 4 Calibration plot of the biosensor. **A** The obtained ECL signals and **B** the plotted ECL intensity vs. Ln (concentration)

It is noted that the linear fitting equation is ($y = -179.93x + 339.28$) R^2 =0.983 which obtained from 1 pg mL^{-1} to 10 ng·mL^{-1} with the limit of detection is 0.6 ng mL^{-1} (S/N = 3).

Compared with most of the other published studies in the literature, the present ECL protocol has a better or comparable LOD with a broad linear range, indicating excellent performance for PSA analysis. Table 1 presents a comparison between our suggested protocol and the other reported bioassays. Thanks to all the scientists whose research has put the spotlight on our achievements, there are some tips and suggestions in this comparison to improve future works. The first tip is LOD which is very important, especially in trace analysis and somehow is a definitive parameter for proposed biosensors. Considering the stronger LOD of other notified papers in Table 1, it should be mentioned that we reported LOD which means practically achieved LOD not theoretically. By the way, the proposed nanobiosensor presented a nice sensitivity toward PSA recognition. The obtained sensitivity is related to the high loading capacity resulting from the CS moieties which hold luminol, AgNPs, and antibodies firmly onto the electrode. The most important achievement of the suggested bioassay is that the proposed biosensor is prepared very rapidly than most other reported research which arises from the fact that electrochemical deposition is much more rapid than the simple drop-casting methods. Also, electrodeposition is a green synthesis method compared to many other preparation techniques with excellent controllability over the resulted films and moieties on the

Table 1 Comparison of the proposed nanobiosensors with previously reported research studies

Modification of electrode	Preparation strategy	Detection method	Incubation/deposition time (min)	LOD (ng·mL^{-1})	LDR (ng·mL^{-1})	Ref
$AgInS_2$ NPs (capture) EDC/NHS, β-CD, NH_2-CuO (probe)	Sandwich type	PEC	Not mentioned DCS, 720 DCS, 120	0.06×10^{-3}	0.1×10^{-3}–100	[27]
AuNPs (capture) $Ni(OH)_2$/NGQDs (capture) Fe_3O_4@MnO_2 (probe)	Sandwich type	ECL	EDP, 30 s Not mentioned Not mentioned	5×10^{-6}	10×10^{-6}–10	[28]
AuNPs (capture) GO-Fe_3O_4-Thi (probe)	Sandwich type	EC	EDP, 5 IMS: 180	0.76×10^{-3}	5×10^{-3}–10	[29]
AuNPs GO@AuNRs/GOD	Sandwich type	ECL	EDP, 30 s 60	0.17×10^{-3}	0.5×10^{-3}–5.0	[30]
AuNPs/rGO Ag+@UIO-66-NH_2/CdWS QDs	Sandwich type	ECL	EDP, 20 DCS, 80	0.038×10^{-3}	0.1×10^{-3}–10	[31]
Au/Ag/rGO-NH_2GQDs/COOH-GQD	Label-free	ECL	DCS, not mentioned	0.29×10^{-3}	1×10^{-3}–10	[32]
AuNPs CS/AgNPs/Lum	Label-free	ECL	EDP, 150 s EDP, 80 s	0.60	10-1 $\times 10^{-3}$	This project

PEC photoelectrochemical, *NHS* N-hydroxysuccinimide, *EDC* 1-(3-dimethylaminopropyl)-3-ethyl-carbodiimide hydrochloride, *β-CD* mono-(6-amino-6- deoxy)-β-cyclodextrin, *DCS* drop-casting, *EDP* electrodeposition, *Thi* thionine, *EC* electrochemical, *IMS* immersing, *GOD* glucose oxidase, *AuNRs* gold nanorods, *GQDs* graphene quantum dots, *rGO* reduced graphene oxide

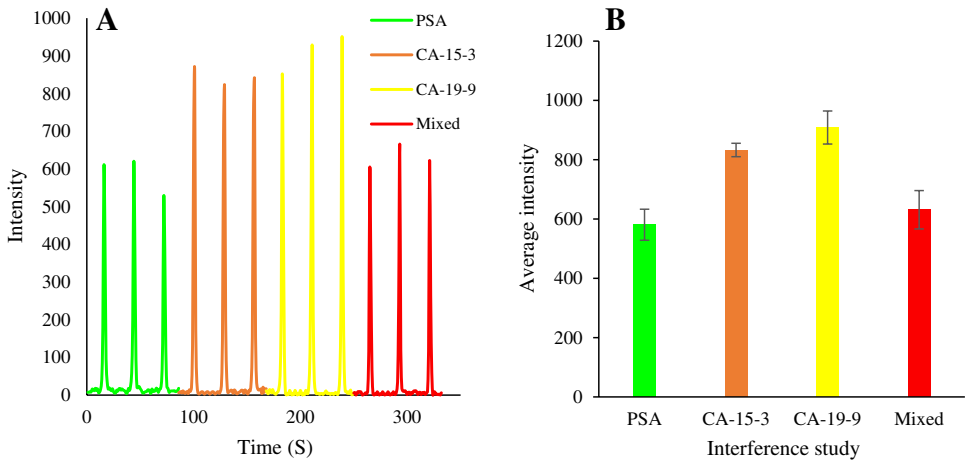

Fig. 5 The specificity of the ECL immunosensor in the presence of PSA, CA-15-3, CA-19-9, and a mix of them. **A** The obtained ECL plots and **B** the correlated histograms (n=3)

electrode. This strategy could bring more repeatability and reproducibility to ECL strategies to be employed in a more accurate and reliable route. To the best of our knowledge, there is no report on electrodeposition of luminol nanocomposite in the literature making the presented methodology novel in this field.

Selectivity

To inform the specificity of the proposed nanobiosensors for PSA against other biomarkers, four possible interferences were selected and tested for the selectivity. In this regard, five discrete solutions of PSA (0.1 ng·mL^{-1}), CA-153 (15 U), CA-19-9 (15 U), CA-125 (15 ng·mL^{-1}), and a mixture solution included PSA, CA-153, CA-19-9, CA-125 (0.1 ng·mL^{-1}, 15 U, 15 U, and 15 ng·mL^{-1}, respectively) were prepared and examined via the nanobiosensor in the optimal conditions. The results were shown in Fig. 5 which indicates a high specificity of the proposed framework toward PSA in the presence of the interferences.

Reproducibility and repeatability

Using three different gold electrodes, three distinct bioassays were prepared at the same conditions as presented in "Electrode preparation steps," and then were employed for 1 ng·mL^{-1} PSA recognition under the same ambient conditions to assess the reproducibility of the method. According to the present data, the relative standard deviation (RSD) was 4.22%, indicating high precision for the immunosensor in detecting PSA with different electrodes. The results were illustrated in Figure S4 **(A-B)**. For repeatability, we recorded the electrical data for one biosensor at the 5 ng ml^{-1} concentration of PSA and the desirable repeatability was obtained as 2.95%.

Table 2 The obtained ECL results and the calculated concentrations with PSA-positive serum samples and recovery percentages

	ELISA	Developed biosensor (n=3)	Recovery %
Sample 1	0.41	0.44	107.31
Sample 2	1.67	1.54	92.21
Sample 3	5.3	5.02	94.71

Stability of the Lum/AgNPs/CS

Furthermore, the ECL stability of the framework has been obtained with no obvious change after cycle 20 (Figure S4-**C**). The electrodeposition of AuNPs and Lum/AgNPs/CS were set at 150 s and 80 s, correspondingly. According to the results, the electrodeposited electroluminophore represents desirable stability against bleaching and releasing from the electrode surface during the ECL measurements.

Real sample analysis

The suggested strategy was also used for screening serum samples (Emam Reza Hospital, affiliated with Tabriz University of Medical Sciences) after the completion of informed consent. For this purpose, after electrodeposition of the AuNPs and CS/AgNPs/luminol consecutively, anti-PSA antibodies were attached to the electrode, as discussed in "Electrodeposition of AuNPs and chitosan/luminol/AgNPs" and "PSA detection procedure." The prepared framework was incubated with untreated serum samples (10 µL) for 2 h to recognize the concentration of PSA protein. To avoid possible errors and interferences, a freshly prepared biosensor was fabricated for each sample. The results are summarized in Table 2. The obtained results by the proposed ECL framework were in agreement with the ELISA data recorded by the clinical setting, representing the applicability for

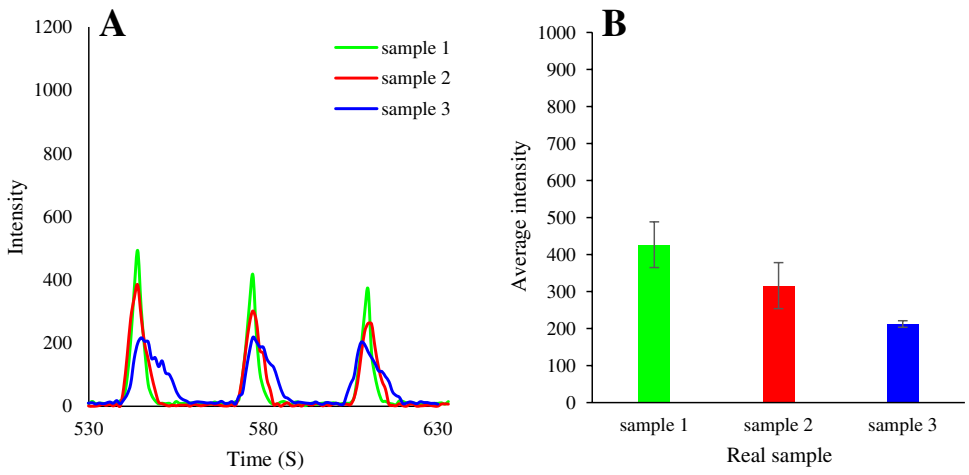

Fig. 6 The analysis of real samples from volunteers with prostate cancer. **A** ECL graphs and **B** the related histograms (n=3)

clinical point-of-care usage. Based on the calibration equation obtained with standard solutions, the concentration of the PSA in real samples was high (1 ng·mL^{-1} and higher) for the carcinoma state, which proved the applicability of the proposed framework in the monitoring of PSA protein and prostate cancer patients (Fig. 6).

It is clear that the proposed method presents good applicability, considering the advantages in the preparation and detection steps as figured in previous sections. Future works should focus on integrating low-cost nanomaterials into the CS-luminol unity to reduce the final costs for large-scale applications. Also, generating new portable tools combined with the advantages of our proposed platform brings benefits for point-of-care diagnostics in clinical settings. In this regard, employing the introduced nanocomposite with screen-printed electrodes with different materials especially paper-based microfluidics provides extraordinary applicability in future studies.

Conclusion

We fabricated a new-style ECL nanobiosensor based on CS-AgNPs-luminol nano-luminocomposite prepared by an electrodeposition protocol for detecting PSA protein in serum samples. Such an operation provides unique advantages over conventional drop-casting of luminophore on the electrode surface, including high uniformity of the luminophore on the electrode, easy preparation, low-consumed time, and producing signals with higher repeatability. It has demonstrated that adding AuNPs increases the nanocomposite's loading capacity, leading to enhanced ECL signals and sensitivity with about two-fold amplification. Trials performed on possible interferences reveal the applicability of the proposed assessment in analyzing untreated serum samples. Such development is able to be exploited in miniaturized ECL systems where drop-casting could be much more complicated. Integrating this protocol with microfluidics and on-chip methods with long-term stability could be the next step in developing this framework, fastening the fabrication of decentralized luminescence biosensors for PSA and other cancer-related proteins.

Supplementary Information The online version contains supplementary material available at https://doi.org/10.1007/s00604-023-05680-8.

Funding Research reported in this publication was supported by Cancer Research Center under award number 29242 and ethical code: IR.SBMU.CRC.REC.1400.032 from the Shahid Beheshti University of Medical Sciences, Tehran, Iran.

Declarations

Conflict of interest The authors declare no competing interests.

References

1. Richter MM (2004) Electrochemiluminescence (ecl). Chem Rev 104(6):3003–3036
2. Gutiérrez-Gálvez L et al (2022) Electrochemiluminescent nanostructured DNA biosensor for SARS-CoV-2 detection. Talanta 240:123203
3. Chenaghlou S et al (2021) Gold nanostar-enhanced electrochemiluminescence immunosensor for highly sensitive detection of cancer stem cells using CD133 membrane biomarker. Bioelectrochemistry 137:107633
4. Isildak I et al (2020) Electrochemiluminescence methods using CdS quantum dots in aptamer-based thrombin biosensors: a comparative study. Microchimica Acta 187(1):1–13
5. Jalili R et al (2022) An electrochemiluminescence biosensor for the detection of Alzheimer's tau protein based on gold nanostar decorated carbon nitride nanosheets. Molecules 27(2):431
6. Nasrollahpour H et al (2021) Homogeneous electrochemiluminescence in the sensors game: what have we learned from past experiments? Anal Chem 94(1):349–365

7. Zanut A et al (2021) DNA-based nanoswitches: insights into electrochemiluminescence signal enhancement. Anal Chem 93(30):10397–10402
8. Nasrollahpour H et al (2021) Ultrasensitive bioassaying of HER-2 protein for diagnosis of breast cancer using reduced graphene oxide/chitosan as nanobiocompatible platform. Cancer Nanotechnol 12(1):1–16
9. Wang Q et al (2021) Ternary electrochemiluminescence biosensor based on DNA walkers and AuPd nanomaterials as a coreaction accelerator for the detection of miRNA-141. ACS Appl Mater Interfaces 13(22):25783–25791
10. Huang L-Y et al (2021) High-performance electrochemiluminescence emitter of metal organic framework linked with porphyrin and its application for ultrasensitive detection of biomarker mucin-1. Sensors Actuators Chem 344:130300
11. Alemu YA et al (2022) Strategies of tailored nanomaterials for electrochemiluminescence signal enhancements. Curr Op Coll Inter Sci p 101621
12. Fathi F, Rahbarghazi R, Rashidi M-R (2018) Label-free biosensors in the field of stem cell biology. Biosens Bioelectron 101:188–198
13. Fathi F et al (2017) Early-stage detection of VE-cadherin during endothelial differentiation of human mesenchymal stem cells using SPR biosensor. Biosens Bioelectron 96:358–366
14. Nasrollahpour H et al (2022) Electrochemical biosensors for stem cell analysis; applications in diagnostics, differentiation and follow-up. TrAC Trends Analytic Chem p 116696
15. Rezabakhsh A, Rahbarghazi R, Fathi F (2020) Surface plasmon resonance biosensors for detection of Alzheimer's biomarkers; an effective step in early and accurate diagnosis. Biosens Bioelectron 167:112511
16. Khalilzadeh B et al (2019) Development of a reliable microRNA based electrochemical genosensor for monitoring of miR-146a, as key regulatory agent of neurodegenerative disease. Intl J Biol Macromol 134:695–703
17. Pourakbari R et al (2019) Recent progress in nanomaterial-based electrochemical biosensors for pathogenic bacteria. Microchimica Acta 186(12):1–13
18. Van Poppel H et al (2021) Prostate-specific antigen testing as part of a risk-adapted early detection strategy for prostate cancer: European Association of Urology position and recommendations for 2021. Eur Urol 80(6):703–711
19. Negahdary M, Sattarahmady N, Heli H (2020) Advances in prostate specific antigen biosensors-impact of nanotechnology. Clinica Chimica Acta 504:43–55
20. Su D et al (2021) Biosensors based on fluorescence carbon nanomaterials for detection of pesticides. TrAC Trends in Analytical Chemistry 134:116126
21. Ma C et al (2019) Recent progress in electrochemiluminescence Sens Imaging. 92(1):431–454
22. Chen X, Liu Y, and QJJoMCC Ma (2018) Recent advances in quantum dot-based electrochemiluminescence sensors. **6**(5) 942-959
23. Nasrollahpour H et al (2021) A highly sensitive electrochemiluminescence cytosensor for detection of SKBR-3 cells as metastatic breast cancer cell line: a constructive phase in early and precise diagnosis. Biosens Bioelectron 178:113023
24. Fan M et al (2021) A versatile chitosan nanogel capable of generating AgNPs in-situ and long-acting slow-release of Ag+ for highly efficient antibacterial. Carbohydr Polym 257:117636
25. Rizwan M et al (2018) AuNPs/CNOs/SWCNTs/chitosan-nanocomposite modified electrochemical sensor for the label-free detection of carcinoembryonic antigen. Biosens Bioelectron 107:211–217
26. Wongpreecha J et al (2018) One-pot, large-scale green synthesis of silver nanoparticles-chitosan with enhanced antibacterial activity and low cytotoxicity. Carbohydr Polym 199:641–648
27. Fu Y et al (2020) Peptide cleavage-mediated and environmentally friendly photocurrent polarity switching system for prostate-specific antigen assay. 93(2):1076–1083
28. Zhu W et al (2018) Ni (OH) 2/NGQDs-based electrochemiluminescence immunosensor for prostate specific antigen detection by coupling resonance energy transfer with Fe3O4@ MnO2 composites 99: p. 346-352
29. Ding C, Wang X, and Luo XJAc (2019) Dual-mode electrochemical assay of prostate-specific antigen based on antifouling peptides functionalized with electrochemical probes and internal references. 91(24): p. 15846-15852
30. Cao JT et al (2018) Graphene oxide@ gold nanorods-based multiple-assisted electrochemiluminescence signal amplification strategy for sensitive detection of prostate specific antigen 99: p. 92-98
31. Fang Q et al (2019) A sensitive electrochemiluminescence immunosensor for the detection of PSA based on CdWS nanocrystals and Ag+@ UIO-66-NH2 as a novel coreaction accelerator. 302: p. 207-215
32. Wu D et al (2016) Label-free electrochemiluminescent immunosensor for detection of prostate specific antigen based on aminated graphene quantum dots and carboxyl graphene quantum dots. 6(1):1–7